

# Hybrid MoM-CG RCS Estimation of Dihedral Corner Reflector

Deepa K. Sasidharan, Subhalakshmy A.B., Vineetha Joy, and Hema Singh\*

Centre for Electromagnetics (CEM), CSIR-National Aerospace Laboratories, Bengaluru-560017, India

\*hemasingh@nal.res.in

**Abstract.** An efficient numerical-based accelerating method for the computation of radar cross section of conducting dihedral corner reflector is presented. The RCS formulation is based on Method of Moments. The integral equation describing the scattering problem is discretized into a set of linear system of equations, which in turn is solved for the equivalent currents defined on the structure via equivalence principle. The equivalent currents thus obtained are further processed to determine the radar cross section. The entire process is further improved in terms of computational memory and time for larger number of unknowns by means of Conjugate Gradient-based accelerating algorithm. The computed results are validated against those obtained through simulation in COMSOL and the measurements.

Keywords: Radar cross section, method of moments, conjugate gradient, dihedral corner reflector

## 1. Introduction

Radar cross section (RCS) [1] can generally be described as the detectability of a target evaluated by means of quantifying the echo signal. It is a measure of the ability of the target to reflect the signal towards the radar receiver. The term RCS is significant especially in stealth aircraft technology where the aircraft should go undetected by the hostile radar. This necessitates the aircraft parts to be manufactured in such a way as to minimize the RCS. Similarly, there are circumstances wherein the RCS of structures needs to be enhanced. In both cases, the prediction of RCS is inevitable and it essentially involves the analysis of scattered fields.

Several high frequency-based, as well as numerical based techniques have been proposed to compute the RCS of various structures. Method of Moments (MoM) [2] is a low-frequency computational method that essentially involves solving the integral form of Maxwell's equations. The technique had been used with Electric Field Integral Equations (EFIE) to analyze the scattering from arbitrary surfaces [3] and scattering patterns could be generated for different structures, for e.g. cylinders of any cross section [4]. One of the main features of MoM is that the method could be applied to any geometry and is also applicable to the inhomogeneous dielectric. The basic procedure of MoM ends up in a system of linear equations that has to be solved for the unknown currents usually through matrix inversion. Although MoM provides considerable flexibility in terms of geometry, it becomes computationally exhaustive for electrically large objects [5]. Thus a powerful computer hardware is required to handle such huge computational memory and time requirement.

In this paper, a hybrid approach combining the Method of Moments with an accelerating Conjugate Gradient (CG) algorithm is applied to compute the RCS of a conducting dihedral corner reflector. This algorithm is introduced to rectify to an extent, the huge computational complexity stated above. The computed results are compared and validated with the simulated results using COMSOL multiphysics simulation tool. One of its add on modules

named RF module is used in RCS calculation, which is based on Finite Element Method (FEM).

A basic dihedral corner reflector is made up of two flat rectangular metal plates connected at right angle to each other, as shown in Figure 1. It is a retroreflector i.e., it reflects back the field directly opposite to the incident direction, thus enhancing RCS. The geometry of a corner reflector provides very large value of RCS for wide range of viewing angles. Hence it finds application in radar calibration and is used as a test target. Moreover, this structure forms a significant part in an aircraft. The tail of an aircraft can be conveniently represented by a dihedral which essentially consists of two flat plates joined at a specific angle. It forms a major contributor towards the RCS of an aircraft along with other parts like fuselage and wings.

## 2. Method of Moments

In problems relating to RCS computation, electromagnetic radiation generated from an external source is incident on the object and currents are generated on them. The generated currents radiate further to give the scattered field.

The technique basically involves formulation of surface integral equation based on surface equivalence principle for a scattering object, then solving for the unknown currents and finally integrating to obtain the scattered field. Most of the complex electromagnetic scattering problems cannot be solved analytically. Such problems, either deterministic or eigenvalue and two or three dimensional electromagnetic scattering problems, are computed numerically.

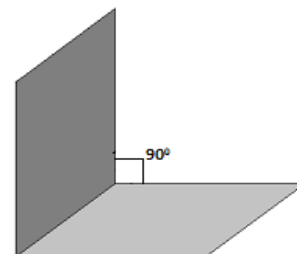


Fig. 1. A basic dihedral corner reflector

2.1. Basic procedure

In the scattering analysis of a perfectly conducting dihedral structure, the Electric Field Integral Equation (EFIE) formulated by applying the boundary conditions and surface equivalence principle is given by [2]

$$-\frac{j}{\omega\mu} \hat{n}(r_o) \times \vec{E}_{inc}(r_o) = \hat{n}(r_o) \times \iint_s G(r_o, r_s) [\vec{J}(r_s) + \frac{1}{k^2} \nabla' \nabla' \cdot (r_s)] dr_s \tag{1}$$

The scattered electric field is given by,

$$\hat{n}(r) \times E_{sca}(r) = -\hat{n}(r) \times E_{in}(r') \tag{2}$$

where  $E_{inc}$  represents the incident field,  $E_{sca}$  represents the scattered field,  $G(r_o, r_s)$  is the Green's function,  $J(r_s)$  the unknown current density and  $r_s, r_o$  are the source and observation points respectively.

The EFIE has to be transformed to a set of homogeneous equations. Initially, the surface of the structure is discretized into a number of patches.

The unknown function is assigned to each cell of the surface patch model. The unknown function in the integral equation is expressed as a weighted sum of basis functions. Following this, the testing functions are incorporated into it. The basis and the testing functions may be either pulse or triangular functions. Finally, a linear system of equations is obtained that could be well represented in matrix form as in Eq. (3) and solved for  $x$ , which will be the unknown current density.

$$Ax = B \tag{3}$$

2.2. Formulation

RCS estimation can be either monostatic or bistatic. Monostatic RCS determination essentially involves both the transmitting and the receiving antennas to coincide with each other, so the scattering analysis is performed for different viewing angles. For bistatic RCS determination, the transmitter is fixed at a certain position, and the receiver is varied along a range of angles. In the present context, the formulation is done for monostatic RCS.

A perfectly conducting dihedral corner reflector with the orientation as given in Figure 2 is the scatterer considered. A plane wave [6] propagating in the z-direction is assumed to be incident on the object and can be mathematically expressed as:

$$\vec{E}_{inc} = e^{jk(x \cos \phi + y \sin \phi)} \hat{z} \tag{4}$$

where,  $\phi$  represents the angle of incidence, and  $\phi$  is varied from  $-180^\circ$  to  $+180^\circ$ . The backscattered field is separately calculated for the incident field vector for each angle.

The total field,  $E_{tot}$  generated due to the source is the sum of incident field,  $E_{inc}$  and scattered field,  $E_{sca}$ .

$$\vec{E}_{tot} = \vec{E}_{sca} + \vec{E}_{inc} \tag{5}$$

For a perfect conductor, the total field on the surface will be zero [7]. The original source is substituted with numerous

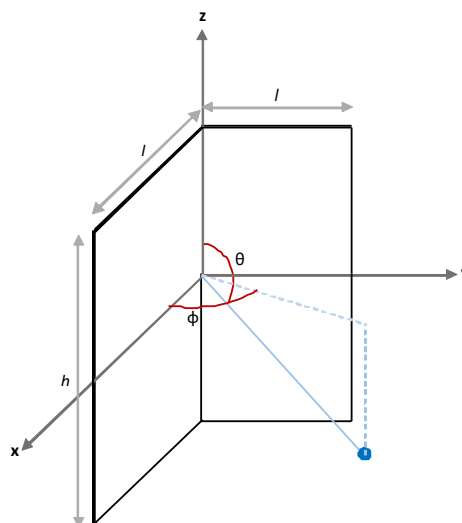


Fig. 2. Dihedral structure-schematic

equivalent sources on the surface according to Huygens' surface equivalence principle.

The scattered field is derived as an integral of Hankel function and the equivalent source field [4].

$$\vec{E}_{sca}(x, y) = - \left\{ \frac{jk^2}{4} \iint (\epsilon_r - 1) E_s(x_s, y_s) H_0^{(2)}(k\rho_{os}) dx_s dy_s \right\} \tag{6}$$

where,  $\epsilon_r$  is the relative permittivity of the material,  $H_0^{(2)}(k\rho_{os})$  represents the Hankel function of second kind and zeroth order, and  $E_s$  represents the unknown source within each cell.

Substituting  $E_{inc}$  and  $E_{sca}$  in Eq. (5), one gets

$$\vec{E}_{tot} + \left\{ \frac{jk^2}{4} \iint (\epsilon_r - 1) E_s(x_s, y_s) H_0^{(2)}(k\rho_{os}) dx_s dy_s = \vec{E}_{inc}(x, y) \right\} \tag{7}$$

In order to solve for the unknowns using MoM, discretization of the structure is performed and equivalent sources are incorporated within each cell. For the dihedral shape, the cross section in the X-Y plane is considered for surface discretization and further formulation.

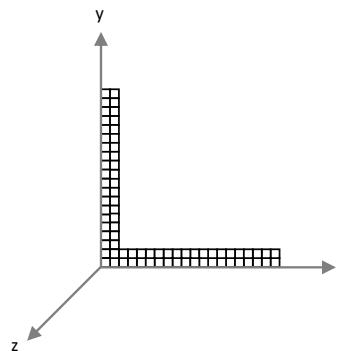


Fig. 3. Discretization of dihedral cross section

The right angled structure is discretized into N number of small square cells (Figure 3), such that the electric field intensity and dielectric constant remains constant within each cell. Since the material is assumed to be homogeneous, the relative permittivity is constant for all the cells. The equivalent sources are assumed to be concentrated at the centre of each cell. If  $(x_s, y_s)$  and  $(x_o, y_o)$  represents the coordinates of source and observation points respectively, the distance between them is given by:

$$\rho_{os} = \sqrt{(x_o - x_s)^2 + (y_o - y_s)^2} \tag{8}$$

Incorporating discretization in Eq. (7), the vector representing the total field in a single cell m due to the sources in all cells can be related as:

$$\left. \begin{aligned} E_m + \left( \frac{jk^2}{4} \right) \sum_{n=1}^N (\epsilon_n - 1) E_n \cdot \iint H_0^{(2)}(k\rho_{os}) dx_s dy_s \\ = E_{m\_inc} \end{aligned} \right\} \tag{9}$$

The expression is simplified to Eq. (10) for the perfectly conducting case by reducing the term  $E_m$  to zero.

$$\left. \left( \frac{jk^2}{4} \right) \sum_{n=1}^N (\epsilon_n - 1) E_n \cdot \iint H_0^{(2)}(k\rho_{os}) dx_s dy_s \right\} = E_{m\_inc} \tag{10}$$

Similarly, the equations can be generated for all the N cells on the structure. The integral of the Hankel function makes the formulation slightly complicated. This could be solved by approximating the discretized cells to be circular. By doing so, a simple form of solution is available for the surface integral of Hankel function of zero-order, which could be directly applied in the formulation. The solution for Hankel function for circular cell is given by:

$$\left. \begin{aligned} \left( \frac{jk^2}{4} \right) \int_0^{2\pi} \int_0^{a_n} H_0^{(2)}(k\rho_{os}) \rho_s d\rho_s d\phi_s \\ = \begin{cases} j \frac{\pi}{2} k a_n H_1^{(2)}(k a_n) + 1 & , m = n \\ \left( j \frac{\pi}{2} k a_n \right) J_1(k a_n) H_0^{(2)}(k \rho_{mn}) & , m \neq n \end{cases} \end{aligned} \right\} \tag{11}$$

The two cases correspond to the relative position of source and observation points, the former corresponds to overlapping points while the latter defines well-separated points. Eq. (10) can thus be represented in a linear form as:

$$\sum_{n=1}^N G_{mn} E_n = E_{m\_inc} \quad m = 1, 2, \dots, N \tag{12}$$

where,

$$G_{mn} = \begin{cases} (\epsilon_r - 1) \left( j \frac{\pi}{2} k a_n H_1^{(2)}(k a_n) + 1 \right) & , m = n \\ \left( j \frac{\pi}{2} k a_n \right) (\epsilon_r - 1) J_1(k a_n) H_0^{(2)}(k \rho_{mn}) & , m \neq n \end{cases}$$

$E_{m\_inc}$  represents the incident wave vector,  $k$  represents the wave number,  $\epsilon_r$  the relative permittivity of the material,  $J_1(k a_n)$  represents Bessel function of first order and  $a_n$  represents the radius of a single circular cell. The unknown vector  $E_n$  that represents scattered field could be solved by matrix inversion. But for larger objects, the number of unknowns would be too large so that the computation becomes complex in terms of memory and computation time. An algorithm could be incorporated to solve them which will be dealt in the next section.

The scattered field determined could be further processed to compute the RCS. The final expression for two-dimensional RCS as a function of azimuthally varying viewing angle,  $\phi$  is given by:

$$\sigma(\phi) = \frac{\pi^2 k}{|E_{inc}|^2} \left| \sum_{n=1}^N (\epsilon_r - 1) E_n a_n J_1(k a_n) e^{jk(x_n \cos\phi + y_n \sin\phi)} \right|^2 \tag{13}$$

The above expression can be used to determine both monostatic as well as bistatic RCS. Monostatic RCS is obtained by following the above steps as such. But for determining bistatic RCS, the incident plane wave is assumed to be fixed at a particular direction ie., the values of  $\theta_{inc}$  and  $\phi_{inc}$  respectively, are made constant. The scattered field for this incident field is calculated over a range of either azimuthal or elevation angles keeping the other term fixed. So bistatic RCS as a function of either  $\theta_{sca}$  or  $\phi_{sca}$  can be plotted.

### 3. Conjugate gradient algorithm

Conjugate Gradient (CG) Method is essentially a non-stationary iterative technique followed accelerating algorithm [8]. The method involves solving the matrix equation,  $Ax=B$ , where  $A$  is the  $N \times N$  Hermitian positive definite vector that corresponds to the term  $G_{mn}$  in Eq. (12),  $x$  is the unknown  $N \times 1$  vector to be determined and  $B$  is the  $N \times 1$  vector describing the incident electric field. Consider a quadratic equation [9],

$$P(x) = c - B^T x + \frac{1}{2} x^T A x \quad , c \in R \tag{14}$$

The objective of CG algorithm is to find a minimum value for  $P$ . So, assuming  $c = 0$  and equating gradient of  $P$  to be zero yields the solution of the matrix equation.

The basic procedure of the CG method is explained in the flowchart shown in Figure 4. The algorithm involves the following computations:

1. Initialization of the unknown vector,  $x_k$ , residual,  $r_k$  and search direction,  $d_0$ :

$$\left. \begin{aligned} x_k &= 0 \\ r_k &= b - Ax_k \\ &= b \\ d_0 &= r_0 \end{aligned} \right\} \tag{15}$$

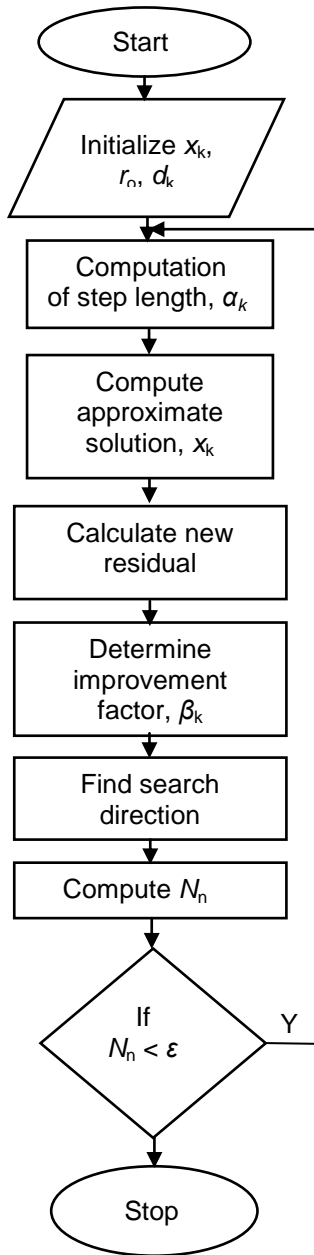


Fig. 4. Conjugate Gradient Method - Flowchart

2. Step length for the next vector solution,

$$\alpha_k = \frac{r_k^T r_k}{d_k^T A d_k} \tag{16}$$

3. Next approximate solution,

$$x_{k+1} = x_k + \alpha_k d_k \tag{17}$$

4. Revised residual,

$$r_{k+1} = r_k - \alpha_k A d_k \tag{18}$$

5. Improvement factor,

$$\beta_k = \frac{r_k^T r_k}{r_{k-1}^T r_{k-1}} \tag{19}$$

6. New search direction,

$$d_k = r_k + \beta_k d_{k-1} \tag{20}$$

7. New deviation,

$$N_n = \frac{\|r_{k+1}\|}{\|b\|} \tag{21}$$

Continue steps 2 to 7 until  $N_n > \epsilon$ . The latest  $x_{k+1}$  will be the required solution. Comparing to Eq. (12),  $x_{k+1}$  correspond to  $E_n$ . Using MoM-CG algorithm, the unknown vector,  $E_n$  is obtained, which can further be employed for RCS computation given in Eq. (13).

#### 4. Results and discussions

Using the above formulation, the monostatic RCS of a perfectly conducting dihedral corner reflector is computed using FORTRAN 90 and validated against simulated results of COMSOL. The material considered is aluminium metal. The scattered fields were analyzed for the TM polarized incident field at viewing angle varying azimuthally from  $-180^\circ$  to  $180^\circ$ . The normalized RCS has been plotted against the azimuthal angle,  $\phi$ .

Results are obtained for different dimensions and frequencies. Figure 5 shows the monostatic RCS of a dihedral corner reflector with length and thickness of the plate is 0.3 m and 0.015 m respectively. A frequency of 9.4 GHz is considered [10]. The computed results are validated against those of COMSOL. It may be observed that both results are in excellent agreement. The corresponding polar plot is depicted in Figure 6.

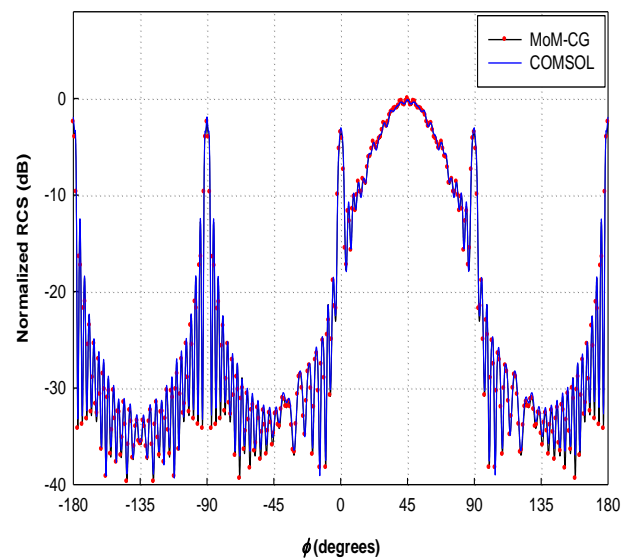


Fig. 5. Normalized RCS of a dihedral at frequency of 9.4 GHz (length of plate = 0.3m, thickness of plate = 0.015m)

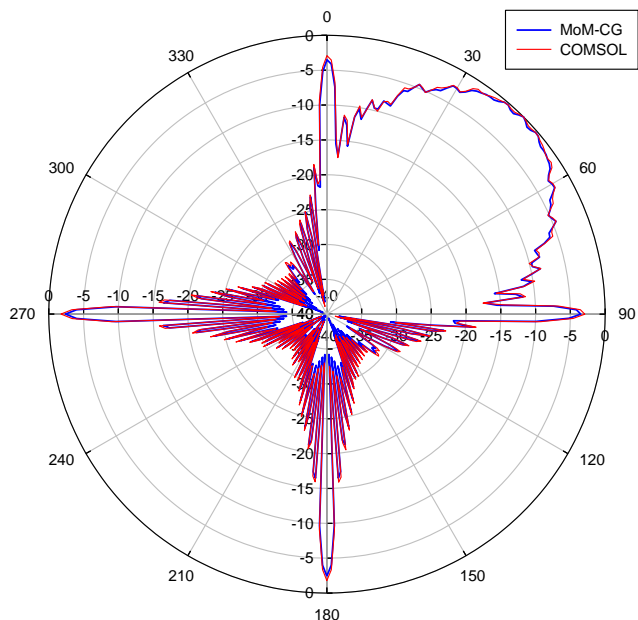


Fig.6. Polar plot showing the normalized RCS of a dihedral at frequency of 9.4 GHz (length of plate = 0.3m, thickness of plate = 0.015m)

Normalized RCS is computed for a dihedral corner reflector of another dimension, 0.3 m × 0.005 m at a frequency of 5 GHz. Figure 7 depicts this plot and its comparison with simulated COMSOL results. Figure 8 shows a comparison between simulated and computed monostatic RCS at 5 GHz for plate length reduced to 0.2 m, while the thickness maintained at 0.005 m.

The computed results show good agreement with simulated results establishing the authenticity of the numerical method employed. The plots show that the RCS is significant for azimuthal angles between 0° and 90° with a maximum at 45°. This region corresponds to the retroreflector. The peaks at 0° and 90° can be attributed to the reflections from edges of the plates. The property of a corner reflector of providing a sharper reflection at the corner is found to be more prominent at higher frequencies.

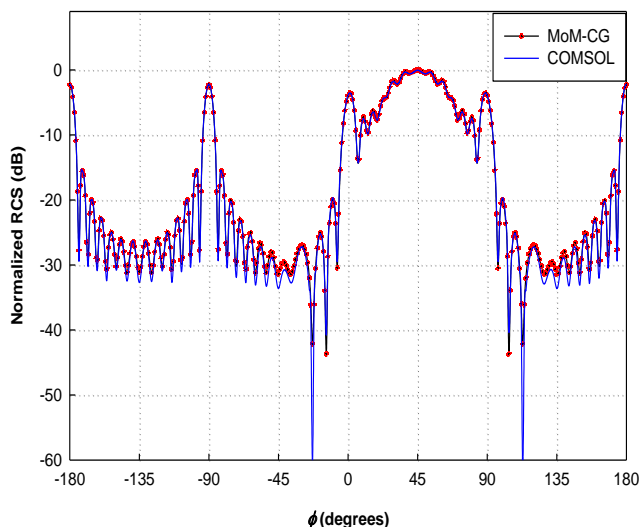


Fig. 7. Normalized RCS of a dihedral at frequency of 5 GHz (length of plate = 0.3 m, thickness of plate = 0.005 m)

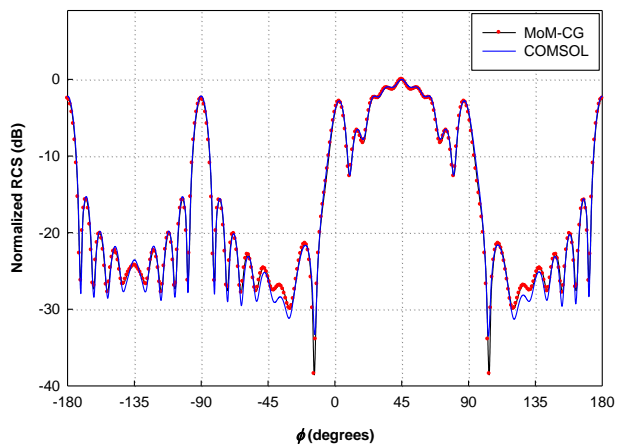


Fig. 8. Normalized RCS of a dihedral at frequency of 5 GHz (length of plate = 0.2 m, thickness of plate = 0.005 m)

The computed result is validated against the experimental [11] results as well. The mismatches in the results are due to errors in the measurement setup. The computed results match excellently with the COMSOL results. Figure 9 shows the comparison among measured, simulated and computed RCS of a dihedral 92° corner reflector made of aluminum with plate dimension of 0.3m × 0.005m at 9.4 GHz frequency. For the analysis, the dihedral structure has been placed in such a way that its two-dimensional cross section lies in the XY plane symmetrical to X-axis. A step size of 4° is considered for the viewing angles ranging between 0° and 360°.

Using MoM-CG formulation, bistatic RCS of a dihedral corner reflector is also computed in FORTRAN 90 and plotted. Figure 10 shows the plot of normalized RCS against scattering angle,  $\phi_{sca}$  for dimensions 0.3m × 0.005m at 9.4 GHz frequency for an incident electric field at  $\theta_{inc} = 0^\circ$ , thereby  $\vec{E} = 1.0$  V/m. Figure 11 shows another plot of normalized RCS for the same dimensions but the incident electric field at  $\theta_{inc} = 90^\circ$  and  $\phi_{inc} = 45^\circ$ . Here the number of discretized cells,  $N$  is taken to be 476. Now, if  $N$  is reduced to 118, the plot will be less accurate as shown in Figure 12. For more precise results, the structure has to be appropriately discretized.

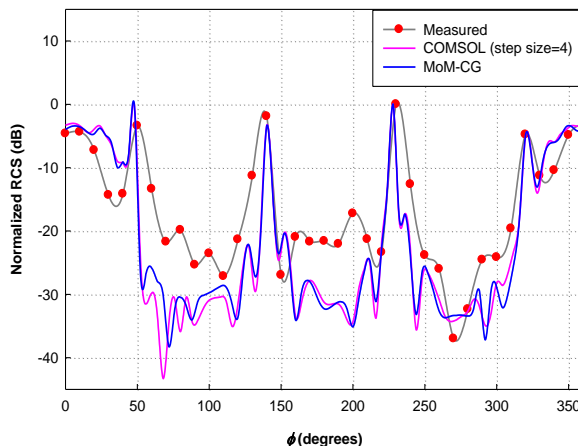


Fig. 9. Normalized RCS of a dihedral at frequency of 5 GHz (length of plate = 0.2 m, thickness of plate = 0.005 m)

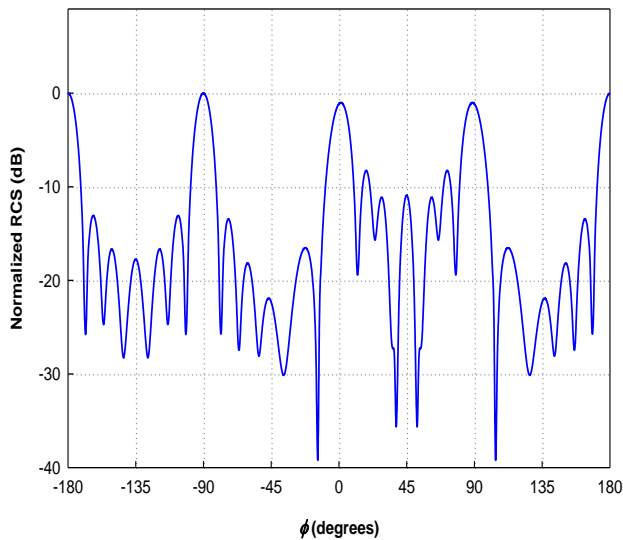


Fig. 10. Normalized Bistatic RCS of a dihedral at frequency of 5 GHz (length of plate = 0.3 m, thickness of plate = 0.005 m) at  $\vec{E}=1.0$  V/m

Table 1 shows the computation time required for the calculating the bistatic RCS of a dihedral structure of dimensions  $0.3\lambda \times 0.002\lambda$  using MoM and MoM-CG for different discretization levels. It is observed that at lower discretization level, there is no significant difference between the time elapsed for both the methods, but as the number of discretized cells are increased, the time requirement become half through the incorporation of the algorithm. So it is clear that MoM-CG is more efficient than MoM especially at higher discretization levels which are required for highly accurate results. The method is found to be more suitable for electrically smaller structures.

For the calculation of monostatic RCS, the computation time depends not only on the number of discretized cells but also on the range of viewing angle and the step size chosen. This is because the solution of the matrix equation has to be calculated for each of the viewing angles and thereby leading to larger number of iterations. So the computation time will be higher for monostatic RCS than bistatic one.

This is clearly shown in Table 2, which illustrates the comparison between the computation time for monostatic and bistatic RCS of a dihedral corner reflector for different discretization levels and range of viewing angle. It is evident that there is a large difference in the elapsed time for bistatic and monostatic RCS computation. The difference is also visible for the same discretization level but different range of angles. The larger time requirement for monostatic RCS can be attributed to the matrix solution calculated for every viewing angle.

The elapsed time increases with increase in the number of equations since the number of unknowns increases affecting the solution of matrix equation to be more complex. The computation time will be even higher with further increase in the extent of discretization. Increasing the step size may help in reducing the computation time but at the cost of accuracy of results.

**Table 1:** Comparison between MoM and MoM-CG for bistatic RCS computation with respect to discretization

Discretization level (Number of equations)	Elapsed Time (in seconds)		Number of iterations (MoM-CG)
	MoM	MoM-CG	
592	1.544	1.544	130
1192	10.686	8.315	188
1792	34.835	22.293	229
2392	81.916	43.165	253
2992	157.046	82.930	316
3592	268.478	121.088	318
4192	423.902	187.186	348

**Table 2:** Comparison between the computation time for calculating monostatic RCS and bistatic RCS using MoM-CG

Discretization level (Number of equations)	Range of Scattering angle	Elapsed Time (in seconds)		Number of iterations (for bistatic RCS)
		Monostatic RCS	Bistatic RCS	
236	(-180°,180°)	11.591	2.184E-2	102
	(-45°,135°)	5.834	2.028E-1	
476	(-180°,180°)	60.185	1.232	165
	(-45°,135°)	20.264	1.186	
716	(-180°,180°)	143.973	3.089	197
	(-45°,135°)	72.852	3.026	
956	(-180°,180°)	266.419	6.099	223
	(-45°,135°)	133.162	6.068	
1196	(-180°,180°)	424.899	10.452	247
	(-45,135)	215.032	10.312	

**5. Conclusion**

The work reported here establishes that MoM-CG is an accurate and an efficient method for the computation of RCS of electrically large structure. The large time requirement that would occur in case of normal MoM implementation has been reduced to a certain extent by using the CG-based accelerating algorithm, where linear equations were solved in an iterative fashion reducing the complexity of matrix inversion. For a conducting dihedral corner reflector, the results obtained numerically are compared with those obtained from simulation and also with experimental results. The computed plots for different frequencies and dimensions are found to match almost exactly with the corresponding simulation results. The method could be extended to other geometries as well.

**References**

[1] E.F. Knott, J.F. Schaeffer and M.T. Tully, *Radar Cross Section*. Scitech Publishing, New York, ISBN: 18911 21251, 611p., 2004.

- [2] W.C. Gibson, *The Method of Moments in Electromagnetics*. Chapman & Hall/CRC, Taylor & Francis Group, ISBN-13: 978-1-4200-6145-1, 272p., 2008.
- [3] S.M. Rao, D.R. Wilton and A.W. Glisson, Electromagnetic scattering by surfaces of arbitrary shape, *IEEE Transactions on Antennas and Propagation*, vol. AP-30, no.3, pp. 409-418, May 1982.
- [4] J.H. Richmond, Scattering by a dielectric cylinder of arbitrary cross section shape, *IEEE Transactions on Antennas and Propagation*, vol. 13, no. 3, pp. 334-341, May 1965.
- [5] A.F. Peterson, S.L. Ray and R. Mittra, *Computational Methods for Electromagnetics*. IEEE/OUP Series on Electromagnetic Wave Theory, ISBN: 978-0-7803-1122-1, 564 p., 1998.
- [6] A.K. Bhattacharya and D.L. Sengupta, *Radar Cross Section Analysis and Control*, Artech House, Boston, London, ISBN: 0-89006-371-0, 289p., 1991.
- [7] C.A. Balanis, *Advanced Engineering Electromagnetics*. NY: John Wiley & Sons, ed. 2, ISBN: 978-0-470-58948-9, 1018 p., 2012.
- [8] G. Strang, *Computational Science and Engineering*. Wellesley-Cambridge Press, United States, ISBN: 9780961408817, 750p., 2007.
- [9] D. Bogusevski, The Buffered Block Forward Backward Technique for Solving Electromagnetic Wave Scattering Problems, Thesis Report, School of Electronic Engineering, Dublin City University, 185p., February 2010.
- [10] T. Griesser, C.A. Balanis and K. Liu, RCS Analysis and Reduction for Lossy Dihedral Corner Reflectors, *Proceedings of the IEEE*, vol.77, no. 5, pp. 806-814, May 1989.
- [11] Z. Haq, *Applied Measurement Systems* InTech Publishing, ISBN:978-953-51-0103-1,390p.,February2012.

#### Biography of the authors



Deepa K. Sasidharan is pursuing M.Tech. (Electronics and Communication) in Cochin University of Science & Technology (CUSAT), Kochi. She is doing her M.Tech. project in Centre for Electromagnetics (CEM) of CSIR-NAL, Bangalore. She obtained her B.Tech. (ECE) degree in 2015 from CUSAT, Kochi. Her research interests include radar cross section (RCS) based studies, and accelerated numerical-based approaches for EM analysis.



Subhalakshmy A.B. obtained her M.Tech. (Electronics and Communication) in 2016 from Cochin University of Science & Technology (CUSAT), Kochi. She obtained her B.Tech. (ECE) degree in 2014 from CUSAT, Kochi. She worked as Project Scientist in Centre for Electromagnetics (CEM) of CSIR-NAL, Bangalore. Her research interests include radar cross section (RCS) based studies, and accelerated numerical-based approaches for EM analysis.



Vineetha Joy is currently working as Scientist at Centre for Electromagnetics of CSIR-National Aerospace Laboratories, Bangalore, India since March, 2016. She obtained B.Tech in Electronics and Communication Engineering with Second Rank from University of Calicut in 2011. She received M Tech degree with First Rank in RF & Microwave Engineering from Indian Institute of Technology (IIT) Kharagpur in 2014. As part of M Tech program, Ms. Vineetha Joy formulated and simulated Propagator Matrix based approach to analyze electromagnetic fields in a cylindrically stratified media, which has potential applications in the analysis of Microstrip Antennas, Dielectric Resonator Antennas, Optical Fibres etc. During 2014-2015, she worked as a research scholar in the Department of Avionics, Indian Institute of Space Science and Technology, Trivandrum, India. The research activities in this tenure were focused on retrieval of electromagnetic parameters of various metamaterial structures and studies on metamaterial cloaks at microwave frequencies with emphasis on Transformation Optics. Ms. Vineetha Joy has presented various research papers in prestigious international symposia and conferences. Her research interests include Computational Electromagnetics, Radar Cross Section Studies, Metamaterials, and Electromagnetic Design and Performance Analysis of Radomes.



Hema Singhis working as Principal Scientist in Centre for Electromagnetics, National Aerospace Laboratories (CSIR-NAL), Bangalore, India. She also holds post of Associate Professor in CSIR Academy, AcSIR. She received Ph.D. degree in Electronics Engineering from IIT-BHU, Varanasi India in Feb. 2000. For the period 1999-2001, she was Lecturer in Physics at P.G. College, Kashipur, Uttaranchal, India. She was a Lecturer in EEE of Birla Institute of Technology & Science (BITS), Pilani, Rajasthan, India, for the period 2001-2004. She joined CSIR-NAL as Scientist in January 2005. She has been a member of IEEE-Industry Initiative Committee, IEEE, IET, IETE, Indian Society for Advancement of Material and Process Engineering (ISAMPE), and Aeronautical Society of India. Her active areas of research and teaching interests are in the domain of: *Computational Electromagnetics* (CEM) for Aerospace Applications, RF and Microwaves. More specifically, the topics of the sponsored projects she has contributed in are Radar Cross Section (RCS) studies including Active RCS reduction, EM analysis of propagation in an indoor environment, phased antenna arrays, adaptive array processing, and conformal array. Dr. Singh has authored or co-authored 11 books, 1 book chapter, 7 software copyrights, 235 scientific research papers and technical reports. She has also supervised over 40 graduate projects and postgraduate dissertations. Dr. Hema Singh received Best Woman Scientist Award in NAL, Bangalore for period of 2007-2008 for her contribution in area of phased antenna array, adaptive arrays, and active RCS reduction.